Informatics in Medicine Unlocked 14 (2019) 6–14

Contents lists available at ScienceDirect

Informatics in Medicine Unlocked

journal homepage: www.elsevier.com/locate/imu

Anti-inflammatory activity screening of *Kalanchoe pinnata* methanol extract and its validation using a computational simulation approach

Happy Agarwal, Venkat Kumar Shanmugam*

School of Bio-Sciences and Technology, Vellore Institute of Technology, Vellore, 632014, TN, India

ARTICLE INFO

Keywords:
Inflammation
Kalanchoe pinnata
In-silico
GCMS
Cytokines
Anti-oxidant

ABSTRACT

Anti-inflammatory activity possessing bio-compounds were identified from *Kalanchoe pinnata* methanolic leaf extract using Gas chromatography-mass spectrometry (GC-MS) analysis and their anti-inflammatory potential was checked using inhibition of albumin denaturation assay, anti-proteinase activity assay, and heat and hypotonicity induced hemolysis assay. GC-MS analysis revealed the presence of aldehydes, ketones, carboxylic acid in the crude. Antioxidant activity analysis using 2, 2-diphenyl-1-picrylhydrazyl (DPPH) assay revealed the half maximal inhibitory concentration (IC_{50}) value of methanol crude leaf extract as 100 μg/mL. The biocompatibility of the methanol extract was determined using 3-(4,5-Dimethylthiazol-2-yl)-2,5-Diphenyltetrazolium Bromide (MTT) assay.

The anti-inflammatory property of identified bio-compounds was also validated using a computational approach. Drug likelihood properties of phyto-compounds were analyzed by predicting the absorption, distribution, metabolism, and excretion (ADMET) score and the bioactivity score. Six chemical compounds with excellent drug relevant properties and availability were selected for a molecular docking study versus a common inflammatory molecular target COX-2 protein. The present study showed that anti-inflammatory properties of phyto-compounds from methanol crude leaf extract of *Kalanchoe pinnata* can be exploited for novel drug design to treat inflammatory disorders.

1. Introduction

Inflammation is a protective immune response towards the invasion of any foreign body such as bacteria, viruses, and parasites [1]. Inflammation research is one of the major fields of global healthcare research, due to the side effects of commercially available non-steroidal anti-inflammatory drugs (NSAIDs), such as renal suppression and gastrointestinal problems like ulcers [2]. Cyclooxygenase-1 (COX-1) and cyclooxygenase-2 (COX-2) are involved in the conversion of Prostaglandin (PGs) to arachidonic acid. COX-2 is generally not found in normal tissues and is only elevated when it is induced by carcinogens or pro-inflammatory cytokines [3]. Recent reports suggested inflammation suppression on selective inhibition of the COX-2 enzyme by natural compounds [4].

Plants are considered as a hub of pharmacologically active bio-compounds and a plethora of plants has been already explored for their anti-inflammatory properties. *Kalanchoe pinnata* has been used in folk medicine since ancient time due to its anti-inflammatory, antibacterial and anti-tumorous activities [5–7].

The present work aims at predicting the bioactive compounds in *Kalanchoe pinnata* methanol extract through GC-MS analysis. The anti-inflammatory activity and antioxidant activity of the methanolic crude leaf extract was investigated and validated through a computational simulation approach. The ADMET property and bioactivity score of the compound was checked to predict drug likelihood properties of selected compounds. Docking analysis was assistive to determine the interaction of active phyto-compounds with active site residues of the COX-2 enzyme. This approach suggests a systematic method for future drug designing using plant active metabolites.

2. Materials and methods

2.1. Plant material collection and storage

Kalanchoe pinnata leaves were collected from Vellore Institute of Technology Campus, Vellore district, Tamil Nadu, India. Fresh leaves were thoroughly cleaned using running tap water and Milli-Q water. Leaves were shade dried, mechanically pulverized, and stored.

* Corresponding author.
E-mail address: venkatkumars@vit.ac.in (V.K. Shanmugam).

https://doi.org/10.1016/j.imu.2019.01.002
Received 10 October 2018; Received in revised form 25 December 2018; Accepted 6 January 2019
Available online 12 January 2019

2.2. Extraction of phyto-compounds

10 g of dried leaf powder was packed with 400 mL of solvent. A sequential non-polar to the polar extraction of phytochemicals was performed using petroleum ether, chloroform, ethyl acetate, and methanol subsequently. Methanolic extract was concentrated under vacuum and reduced pressure using a rotary evaporator at 60 °C. Crude extract obtained after complete drying was used for GC-MS analysis and anti-inflammatory activity screening.

2.3. Phyto-compound identification through GC-MS analysis

The GC-MS analysis was carried out to profile the pharmacologically active constituent present in methanolic leaf extract. The analysis was conducted using Thermo GC - trace ultra VER: 5.0, Thermo MS DSQ II spectrometer. The initial temperature of 70 °C was maintained for 2 min, which was further increased to 260 °C at the rate of 6 °C/min, and was held for 9 min. Helium was used as a carrier gas and a flow rate of 1 mL/min was maintained. 1 μL of the extract was used as a sample injection volume. The total run time was 15.3 min for petroleum ether extract, 15.1 min for ethyl acetate extract, and 16.1 min for chloroform extract. The National Institute of Standards and Technology (NIST) library was screened as a reference for mass spectrometric major peaks evaluation. The percent yield of the extract was also quantified as 0.43%.

2.4. In-vitro anti-inflammatory activity screening of phyto-compounds

2.4.1. Inhibition of albumin denaturation assay

2 mL of 1% Bovine serum albumin (BSA) was mixed with 400 μL of methanolic crude extract in different concentrations (500-100 μg/mL) and the pH of the reaction mixture was adjusted to 6.8 using 1N HCl. The reaction mixture was incubated at room temperature for 20 min and then heated to 55 °C for 20 min in a water bath. The mixture was cooled to room temperature and the absorbance value was recorded at 660 nm. A BSA mixture with 30% methanol solution was used as a control. Diclofenac sodium in different concentrations was used as a standard [8,9]. The experiment was performed in triplicate.

Percent inhibition was calculated using the following formula:

$$\% \text{ Inhibition } = \frac{\text{Control O.D} - \text{sample O.D}}{\text{Control O.D}} * 100$$

Where,

Control O.D = Optical density of control
Sample O.D = Optical density of test sample

2.4.2. Anti-proteinase activity assay

1 mL of 20 mM Tris HCl buffer (pH 7.4) was mixed with 0.06 mg of trypsin and 1 mL of extract in different concentrations (100–500 μg/mL). The reaction mixture was incubated at room temperature (37 °C) for 5 min. 0.8% casein was added to the reaction mixture and was further incubated for 20 additional minutes. Two ml of 70% perchloric acid was added to the mixture to terminate the reaction. The solution was centrifuged at 3000 rpm for 10 min. The absorbance of the supernatant was recorded at 210 nm. Diclofenac sodium in different concentrations was used as a standard. The IC_{50} value was calculated. The experiment was performed in triplicate.

Percent inhibition was calculated using the following formula:

$$\% \text{ Inhibition } = \frac{\text{Control O.D} - \text{sample O.D}}{\text{Control O.D}} * 100$$

2.4.3. Membrane stabilization assay

2.4.3.1. Preparation of R.B.C suspension. A blood sample was centrifuged at 3000 rpm for 10 min and washed thrice with normal isotonic saline. 10% (v/v) normal saline was added to the tubes and this was stored at 4 °C for further experimental use.

2.4.3.2. Heat-induced hemolysis assay. 1 mL of 10% (v/v) R.B.C suspension was mixed with 1 mL of plant extract (100–500 μg/mL). The reaction mixture was incubated in a water bath at 56 °C for 30 min. The tubes were cooled to room temperature under running tap water. The tubes were centrifuged at 2500 rpm for 5 min and the absorbance value of supernatant was determined spectrophotometrically at 560 nm. Diclofenac sodium was used as a standard. The percentage inhibition of hemolysis was calculated as follows:

$$\% \text{ Inhibition } = \frac{\text{Control O.D} - \text{sample O.D}}{\text{Control O.D}} * 100$$

2.4.3.3. Hypotonicity induced hemolysis assay. 1 mL of plant extract (100–500 μg/mL) was added to an equal volume of P.B.S (phosphate buffer saline), 2 mL of hyposaline and 0.5 mL of HRBC suspension. The reaction mixture was incubated at 37 °C for 30 min. The reaction mixture was further centrifuged at 3000 rpm and the absorbance of the supernatant was measured at 560 nm.

$$\% \text{ Inhibition } = \frac{\text{Control O.D} - \text{sample O.D}}{\text{Control O.D}} * 100$$

2.5. Anti-oxidant activity

2 mL of plant extract in the concentration range of 10–300 μg/mL was prepared in 50% methanol solution and was added to an equal volume of 0.1 mM of DPPH solution. The reaction mixture was incubated for 30 min in a dark enclosure at room temperature. The absorbance value was measured spectrophotometrically at 517 nm. The methanol solution was used as a blank. A methanol solution mixed with 0.1 mM of DPPH solution was used as a control. Ascorbic acid was used as a standard. The IC_{50} value was calculated. The percent inhibition was calculated using the formula

$$\% \text{ Inhibition } = \frac{\text{Absorbance of control} - \text{ Absobance of Sample}}{\text{Absorbance of control}} * 100$$

2.6. Cell culture

Raw 264.7 cell lines were procured from the National center for cell lines (NCCS, Pune, India). Cells were cultured in Dulbecco's modified Eagle medium (DMEM) media, supplemented with 10% FBS and 1% penicillin-streptomycin, and maintained at 37 °C in a 5% CO_2 humid atmosphere. Passage no. 17 was used for the assay.

2.6.1. Cell viability assay

The MTT assay was used to evaluate the effect of the extract on cell viability. Cells (3* 10^4) were seeded in a 96 well plate and grown for 24 h. Cells were further treated with different concentrations of extract (20, 10, 5, 2.5, 1.25 μg/mL in 0.1% dimethyl-sulfoxide) and after a 24 h incubation, 20 μL of 5 mg/mL MTT solution in PBS was added to each well. Formazan crystals were dissolved in 100 μL of DMSO after another 4 h incubation period, and the optical density was recorded at 490 nm using a microplate reader. Untreated cells were used as a control.

2.7. Virtual screening of phyto-compounds ADMET property and bioactivity score

SMILES notations of all of the phyto-compounds predicted using GC-MS spectra were either derived from the PubChem database or generated using Marvinsketch version 15.6.8 and were input online to Molinspiration cheminformatics software version 2011.06 (www.molinspiration.com) for ADMET properties and bioactivity score

prediction [10]. Drug-likeness properties including topological polar surface area (TPSA), octanol/water partition coefficient (Log P), number of hydrogen bond donors (NH and OH groups) and acceptors (mostly N and O groups), number of atoms, molecular weight, and number of rotatable bonds were calculated to justify the oral application of the compounds. The bioactivity score for potential targets such as kinase inhibitors, GPCR ligands, enzymes, and nuclear receptors and ion channel modulators were calculated.

2.8. Molecular docking study

2.8.1. Ligand generation and optimization

The two-dimensional structures of Palmitic acid (PubChem ID 985) and Photocitral A (PubChem ID 102684) were downloaded from the PubChem database in .sdf format. The structure of the other four compounds was drawn using Marvinsketch version 15.6.8. Marvinsketch is a chemical editor tool with rich editing features such as 3D editing, 2D cleaning and conformation generation, drawing and formatting shapes, and structure annotation [11].

All of the ligand structures were converted into 3D, and their geometry was optimized before docking using VEGA ZZ version 3.1.1 software [12]. VEGAZZ is a molecular modeling software which allows the visualization of the molecule in multiple file formats, conformation and molecular dynamics trajectory analysis of the molecule. VEGAZZ has an integrated molecular energy minimization tool provided by AMMP, which employs various energy minimization algorithms like steepest descent, conjugate gradient, and genetic algorithm among many others [13]. Hydrogen bonds were added followed by Gasteiger charge addition, energy minimization using AMMP, and structure validation using Mopac tool version 7.01–4 integrated into VEGA ZZ version 3.1.1 software [14]. MOPAC is a computer program used for running semiempirical calculations for structure optimization of small compounds [15].

2.8.2. Target preparation

The three-dimensional structures of the inflammatory receptor target COX-2 were retrieved from the Protein data bank (PDB) database in .pdb format (PDB ID: 5IKR). All of the ligands and water molecules were removed from the protein molecule prior to docking.

2.8.3. Active site prediction

Active pockets of COX-2 protein molecule were determined using the online tool Computed Atlas of Surface Topography of proteins (CASTp 3.0- http://sts.bioe.uic.edu/castp/), and docking was performed versus the binding site in the pocket. CASTp is a webserver that provides geometric and topological information about the protein such as surface pockets, functional sites, details of the pocket including its surface area, volume, and interior cavities [16]. These pockets provide active sites of a protein molecule to perform functions like ligand binding and enzymatic interaction.

2.8.4. Molecular docking

Phyto-compounds were docked against the inflammatory receptor using the AutoDock 4.2 tool, and the binding scores were calculated [17]. AutoDock is a user-friendly, most widely used software to dock small compounds against specific proteins. Polar hydrogen was added to the protein and merged with non-polar hydrogens followed by Kollman charges addition. The grid parameter was set to (80*80*80) and the grid box covered all the active sites in the binding pocket. The Lamarckian genetic search algorithm was used, and docking runs were set to 10. Confirmation energy, ligand efficiency, and inhibitor constant (K_i) were evaluated, and best fit docked structure was visualized using the PyMOL viewer. Interacting residues of the protein forming hydrogen bond with compounds were seen in the PyMOL viewer, and the hydrophobic residue interaction was analyzed using LigPlot version 2.1 [18]. LigPlot provides a schematic 2-D representation of the interaction between protein and the ligand molecule. LigPlot representation reveals hydrophobic bonds, a hydrogen bond with its length and atoms involved in the formation of hydrophobic linkage, and Vander wall interactions between the ligand and protein.

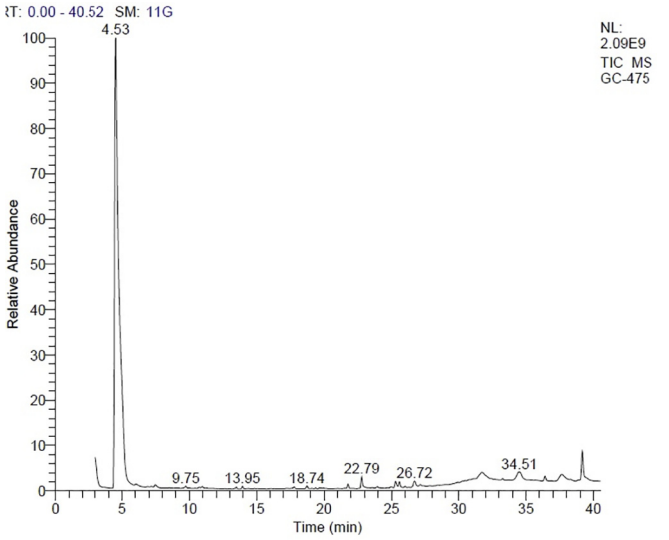

Fig. 1. GC spectra of *Kalanchoe pinnata* methanol crude extract.

3. Results and discussion

3.1. GC-MS analysis

The percent yield of the methanol extract was found to be 0.5%. Fig. 1 reveals the major peak found in the methanol extract, and the NIST Library was referred for the identification of each compound, based upon the peak area and the retention time in the chamber. Bioactive compounds present in the methanol extract of *Kalanchoe pinnata* are shown in Table 1. Based on the area percent, major compounds present in the extract were identified as methane, sulfinylbis- (CAS); 4á,5à-dimethyl-3-methylene-1-azabicyclo[3.2.0]heptan-7-one and hexadecanoic acid (CAS) respectively. Molecular formulae, molecular weight, and area percent of the major compounds are also presented in the table. methanol extract depicted the extraction of many polar compounds like carboxylic acid (Hexadecanoic acid), aldehyde (Photocitral A) and ketones (5-Isopropyl-4-(trifluoromethyl)-1H-pyrimidin-2-one; 1-Benzyl-3-isopropyl-5-(1-allylindol-3-yl)-5-t-butyloxy carbonylpyrrole-3-one; 4á,5à-dimethyl-3-methylene-1-azabicyclo [3.2.0] heptan -7-one). Approximately the same retention time peaks have been already reported in previous literature [19].

3.2. Anti-inflammatory activity screening of plant extract

3.2.1. Inhibition of albumin denaturation assay

Protein denaturation is a well-implicated cause leading to the inflammatory response of cells [20]. BSA was used as a reagent for the assay. 60% of total protein content in animal serum is constituted from BSA alone, and is commonly used in cell culture, particularly when protein supplementation is necessary and the other components of serum are unwanted. BSA undergoes denaturation when exposed to heat, and expresses antigens associated with Type III hypersensitive reaction, which are related to diseases such as glomerulonephritis, rheumatoid arthritis, systemic lupus erythematosus, and serum sickness [21]. Thus, inhibition of BSA denaturation assay was used to evaluate the anti-inflammatory potential of the methanolic crude extract of *Kalanchoe pinnata*.

The extract represented dose-dependent inhibition of BSA

Table 1
Biological active compounds derived from *Kalanchoe pinnata* methanol leaf extract.

S.No.	Retention time (min)	Compound name	Canonical Smiles	Peak area (%)	Molecular formulae	Molecular weight
1	4.51	Methane, sulfinylbis- (CAS)	CS(C)=O	79.19	C_2H_6OS	78
2	9.75	Trans-2,4-Dimethylthiane, S,S-dioxide	CC1CCS(=O)(=O)C(C)C1	0.36	$C_7H_{14}O_2S$	162
3	13.95	5-Isopropyl-4-(trifluoromethyl)-1H-pyrimidin-2-one	CC(C)C1=CNC(=O)N=C1C(F)(F)F	0.30	$C_8H_9F_3N_2O$	206
4	18.74	Photocitral A	CC1CCC(C1C=O)C(C)=C	0.40	$C_{10}H_{16}O$	152
5	22.79	Hexadecanoic acid (Palmitic acid)	CCCCCCCCCCCCCCCC(O)=O	1.37	$C_{16}H_{32}O_2$	256
6	26.72	1-Benzyl-3-isopropyl-5-(1-allylindol-3-yl)-5-t-butyloxy carbonylpyrrole-3-one	CC(C)C1=CN(CC2=CC=CC=C2)C(C(=O)OC(C)(C)C)(C1=O)C1=CN(CC=C)C2C=CC=CC=C12	1.13	$C_{30}H_{34}N_2O_3$	470
7	34.51	4à,5à-dimethyl-3-methylene-1-azabicyclo[3.2.0]heptan-7-one	CC1C(=C)CN2C(=O)CC12C	2.01	$C_9H_{13}NO$	151

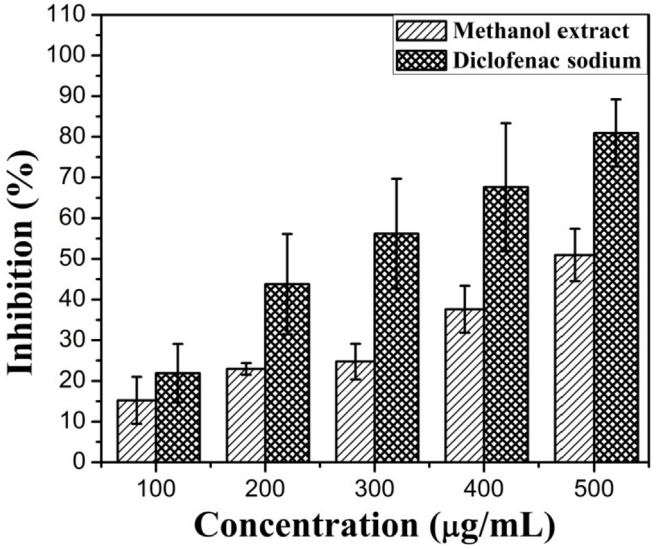

Fig. 2. *Kalanchoe pinnata* methanol extract effect on albumin denaturation.

denaturation. The IC_{50} value was determined to be 490 µg/mL respectively. The IC_{50} value obtained for the standard drug was 250 µg/mL (Fig. 2).

3.2.2. Anti-proteinase activity

Neutrophils are a rich source of serine proteinases and are known to be involved in inflammatory reactions. Their contribution has been reported in the pathology of arthritis [22]. Casein was used as a substrate and trypsin was used as a serine protease enzyme to cleave the peptide linkage of casein. The extracts demonstrated concentration-dependent anti-proteinase activity, and the results were comparable to the standard drug at higher concentrations. The IC_{50} value obtained from methanol extract was 350 µg/mL and the diclofenac sodium IC_{50} value was found to be 300 µg/mL (Fig. 3).

3.2.3. Membrane stabilization assay

The human red blood cell (HRBC) membrane is analogous to the lysosomal membrane in terms of its integrity, and thus it is used to measure the membrane stabilizing capacity of the extract. It is presumed that if extract can stabilize HRBC membrane, it could prevent

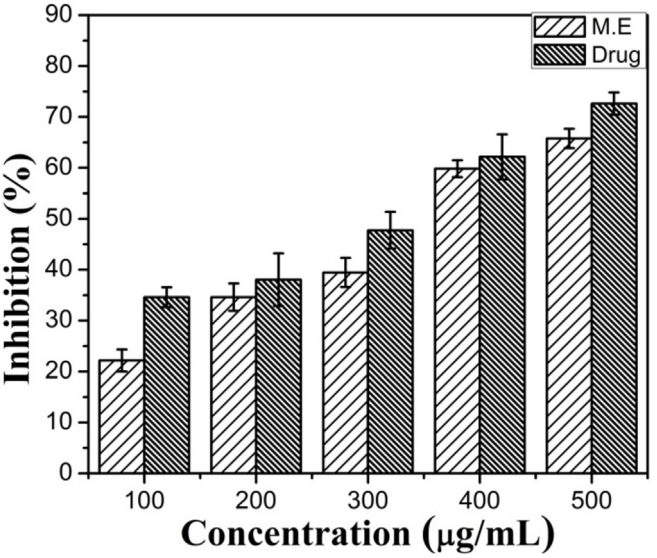

Fig. 3. Anti-proteinase activity of *Kalanchoe pinnata* methanolic crude extract [M.E – methanol extract; Drug- Diclofenac sodium].

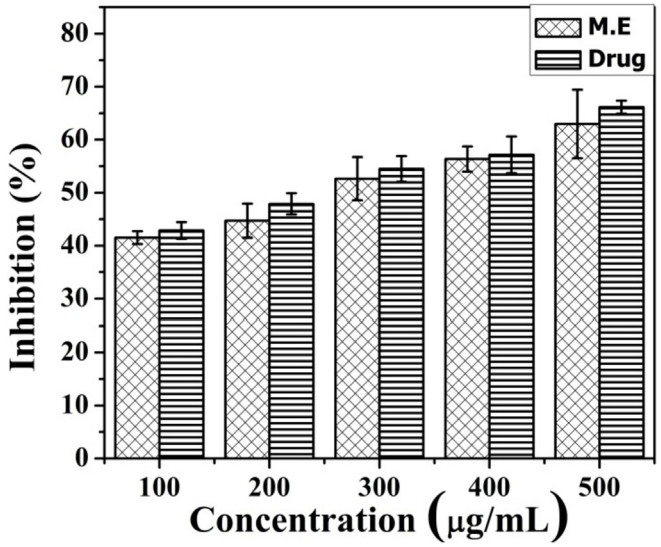

Fig. 4. *Kalanchoe pinnata* methanolic extract effect on heat-induced hemolysis.

the release of a lysosomal enzyme. Heat and hypotonicity cause membrane lysis accompanied by hemoglobin oxidation, and thus membrane stabilization against heat and hypotonicity-induced lysis was used as a measure to study the anti-inflammatory effect of extracted crude compounds [23].

3.2.3.1. Heat-induced hemolysis assays. Methanol extracts represented dose-dependent inhibition and the percent inhibition was similar to the standard drug used, i.e. diclofenac sodium. The IC_{50} value of the extracted crude was found to be 280 µg/mL while the drug depicted more potency with an IC_{50} value of 250 µg/mL (Fig. 4).

3.2.3.2. Hypotonicity induced hemolysis assay. Hypotonicity induced hemolysis is caused by excessive fluid accumulation inside the cell, which makes the cell more susceptible to free radical induced secondary damage, and lipid peroxidation [24]. The methanol extract of *Kalanchoe pinnata* effectively inhibited the hypotonicity-induced hemolysis of HRBC at different concentrations (100–500 µg/mL) as shown in Fig. 5. The percent inhibition by methanol crude extract and drug suggested the IC_{50} value for both to be $<$ 100 µg/mL (Fig. 5).

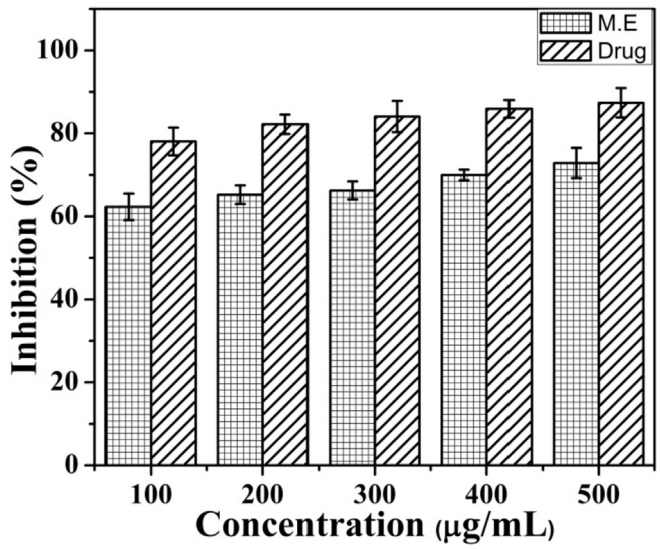

Fig. 5. *Kalanchoe pinnata* methanolic extract effect on hypotonicity-induced hemolysis.

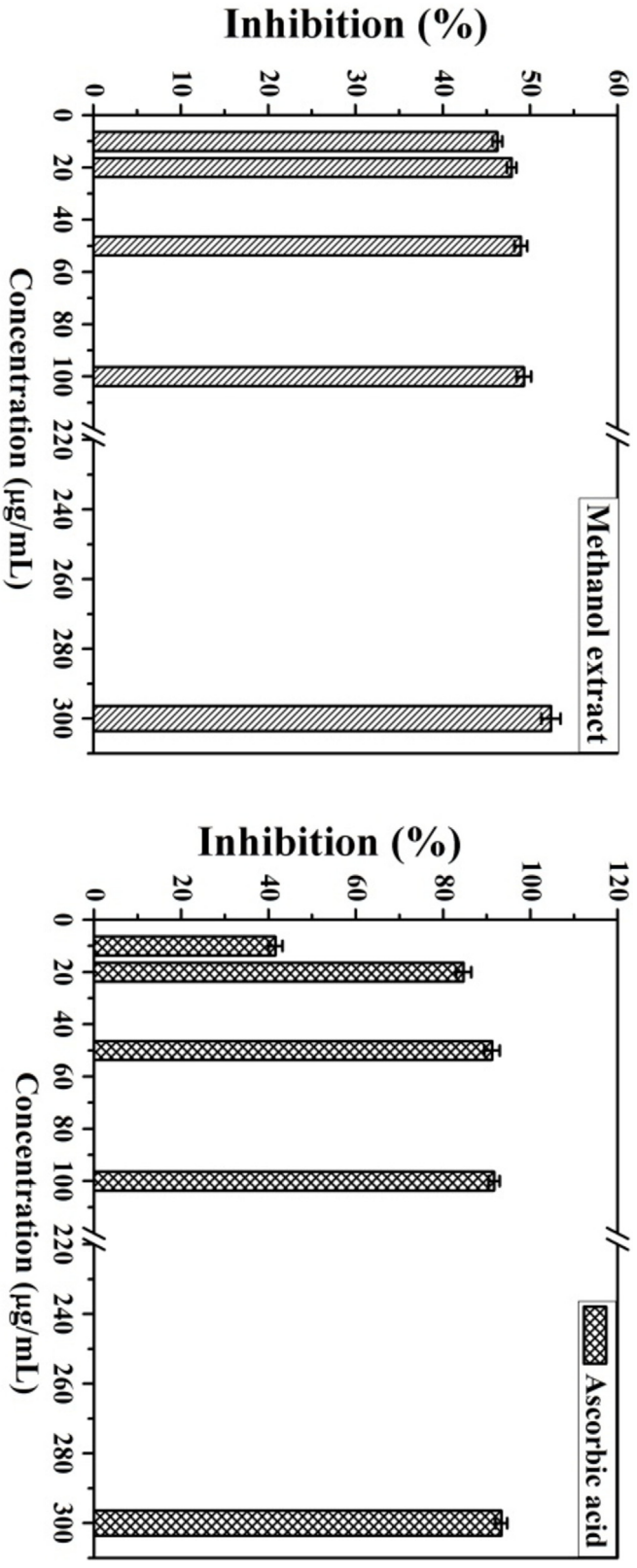

Fig. 6. Anti-Oxidant activity of *Kalanchoe pinnata* methanol crude extract.

3.2.4. Anti-Oxidant activity

The antioxidant potential of plant crude extract was assessed by the DPPH radical scavenging assay. Antioxidant donates a free electron to DPPH-, a stable purple colored lipophilic free radical. The purple color changes to pale yellow gradually, and changes in absorbance at 517 nm

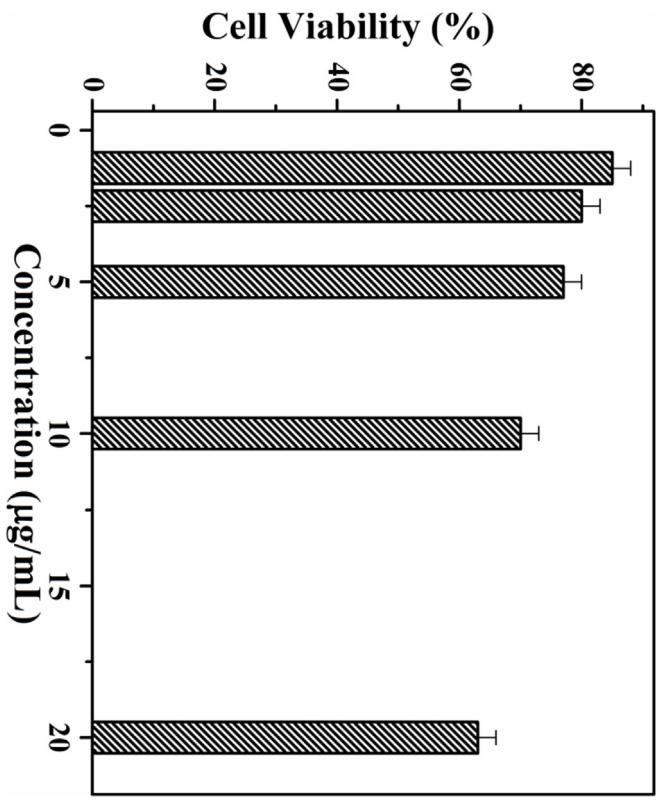

Fig. 7. The effect of methanol extract on cell viability.

will follow [25,26]. The results demonstrated that methanol crude extract of *Kalanchoe pinnata* fresh leaf extract had the capacity to donate hydrogen to the free radical and remove an odd electron. The IC_{50} value obtained from methanol extract was found to be 100 µg/mL, and for Ascorbic acid, it was reported to be 15 µg/mL (Fig. 6).

3.2.5. Cell viability assay

The cytotoxicity of extract in different concentrations (20, 10, 5, 2.5, 1.25 µg/mL) was determined using the MTT assay. The control value was considered as 100% for the cell viability calculation on exposure to extract. The extract did not kill cells, even in higher concentrations, showing their non-cytotoxic nature (Fig. 7).

3.3. In silico analysis

In-silico studies were conducted in order to screen out phyto-compounds with better bioavailability, drug likeliness properties, and greater affinity towards the pro-inflammatory gene, viz. COX-2.

3.3.1. ADMET property and bioactivity score prediction

Prediction of ADMET properties provides insight into possible pharmacokinetics and pharmacodynamics of the compound [27]. All of the compounds met Lipinski's rule of five criteria, as their molecular weight was < 500 Da, number of hydrogen bond donors < 5, hydrogen bond acceptor number < 10, and Log P value < 5 [28]. The log P value of the molecule is related to intestinal absorption, transport through membrane, metabolism, and toxicity. Palmitic acid is expected to have maximum lipophilicity, as its log P value was more than 5, while methane, sulfinylbis- (CAS) is expected to have the highest hydrophilicity as its log P value was −0.69. This implies that Palmitic acid will have poor aqueous solubility and dissolution, while permeation through biomembranes will be the limiting factor for Methane, sulfinylbis- (CAS). TPSA calculates the sum of surfaces of polar atoms like Hydrogen, Nitrogen, and Oxygen in a molecule, which plays a very important role in drug absorption through the human intestinal layer, and drug penetration through the blood-brain barrier. The TPSA value clearly depicts that the hydrogen-bonding capacity of 1-Benzyl-3-isopropyl-5-(1-allylindol-3-yl)-5-t-butyloxy carbonylpyrrole-3-one is a maximum and thus, it is likely to have better bioavailability and membrane transport properties. A number of rotatable bonds indicated the more flexible nature of Palmitic acid as compared to other compounds (Table 2). A number of hydrogen bond donors and acceptors are within the range of Lipinski's rule for all seven compounds. A small molecule with large surface area interacts with water efficiently, and permits better absorption of the drug. The molecular weight of all seven compounds was found to be below 500 Da, indicating that they could be easily transported, diffuse across the cell membrane, and absorbed. Palmitic acid violates 1 Lipinski's rule (log p-value should be less than 5) but still can be considered as a suitable drug candidate [29].

Table 3 summarizes the bioactivity score of the predicted phyto-compounds. A larger bioactivity score suggests better activity. Compounds having a bioactivity score more than 0.00 are assumed to have considerable effect, between −0.50 and 0.00 they are expected to have a moderate effect, and below −0.50 they are assumed to be inactive [29,30]. The bioactivity score for the GPCR ligand was found to be maximum for 1-Benzyl-3-isopropyl-5-(1-allylindol-3-yl)-5-t-butyloxy carbonylpyrrole-3-one, indicating its strong interaction with the ligand. The Photocitral A bioactivity score demonstrates its moderate interaction affinity for ion channels, nuclear receptors, and moderate enzyme inhibition activity. Since their scores are between −0.5 and 0. Palmitic acid exhibits a strong enzyme inhibitory action, interaction with GPCR ligand and nuclear receptor ligand. Palmitic acid also is shown as an effective ion channel modulator and as an effective enzyme inhibitor. All of the compounds could be used as potent anti-inflammatory drug molecules, as they show a promising bioactivity score and follow the Lipinski's rule of 5.

3.3.2. Docking studies

Surface area, volume of the pocket was found to be 1785.762 and 1369.030 respectively, and the atoms that fall under this pocket size were identified as 34ASN, 36CYS, 39HIS, 40PRO, 41CYS, 42 GLN, 43 ASN, 44 ARG, 45 GLY, 46 VAL, 47 CYS, 48 MET, 49SER, 58 ASP, 60THR, 61ARG, 62THR, 63GLY, 64PHE, 76THR, 79LYS, 80LEU, 83LYS, 84PRO, 86PRO, 89VAL, 90HIS, 93LEU, 112ILE, 113MET, 115TYR, 116VAL, 118THR, 119SER, 120ARG, 121SER, 122HIS, 123LEU, 124ILE, 125ASP, 126SER, 127PRO, 128PRO, 129THR, 130TYR, 132ALA, 133ASP, 134TYR, 135GLY, 136TYR, 137LYS, 149THR,

Table 2
Drug likeness score of compounds.

SI.No.	Compound name	Log P	TPSA	nAtoms	nON	nOHNH	n violation	n rotb.	Volume	MW
1	Methane, sulfinylbis- (CAS)	−0.69	17.07	4	1	0	0	0	71.43	78.14
2	Trans-2,4-Dimethylthiane, S,S-dioxide	1.23	34.14	10	2	0	0	0	150.41	162.25
3	5-Isopropyl-4-(trifluoromethyl)-1H-pyrimidin-2-one	1.81	45.75	14	3	1	0	2	165.10	206.17
4	Photocitral A	3.21	17.07	11	1	0	0	2	165.72	152.24
5	Palmitic acid	7.06	37.30	18	2	1	1	14	291.42	256.43
6	1-Benzyl-3-isopropyl-5-(1-allylindol-3-yl)-5-t-butyloxy carbonylpyrrole-3-one	4.54	49.85	35	5	0	0	9	461.33	472.63
7	4á,5à-dimethyl-3-methylene-1-azabicyclo[3.2.0]heptan-7-one	1.42	20.31	11	2	0	0	0	150.51	151.21

Table 3
Bioactivity score of the compounds according to Molinspiration Cheminformatics software.

SI.No.	Compound name	GPCR ligand	Ion channel modulator	Kinase inhibitor	Nuclear receptor ligand	Protease inhibitor	Enzyme inhibitor
1	Methane, sulfinylbis- (CAS)	−3.72	−3.85	−3.85	−3.70	−3.64	−3.65
2	Trans-2,4-Dimethylthiane, S,S-dioxide	−1.35	−1.19	−1.82	−1.64	−0.85	−0.77
3	5-Isopropyl-4-(trifluoromethyl)-1H-pyrimidin-2-one	−0.45	−0.59	−0.87	−0.56	−1.05	−0.30
4	Photocitral A	−0.89	−0.34	−1.79	−0.22	−0.71	−0.27
5	Palmitic acid	0.02	0.06	−0.33	0.08	−0.04	0.18
6	1-Benzyl-3-isopropyl-5-(1-allylindol-3-yl)-5-t-butyloxy carbonylpyrrole-3-one	0.13	0.01	−0.26	0.12	0.18	0.03
7	4á,5à-dimethyl-3-methylene-1-azabicyclo[3.2.0] heptan-7-one	−0.77	−0.37	−1.53	−1.08	−0.66	−0.51

Table 4
Docking analysis of predicted phytochemical from the methanol extract of *Kalanchoe pinnata* leaf with COX-2 protein.

SI.No.	Compound name	Binding score (Kcal/mol)	ligand efficiency	inhibitor constant (K_i)	Interacting residues
1	Trans-2,4-Dimethylthiane, S,S-dioxide	−6.33	−0.63	22.83	TRP387
2	5-Isopropyl-4-(trifluoromethyl)-1H-pyrimidin-2-one	−5.19	−0.37	155.73	GLN42
3	Photocitral A	−6.36	−0.58	21.91	TRP 387
4	Palmitic acid	−6.0	−0.33	40.31	LYS137
5	1-Benzyl-3-isopropyl-5-(1-allylindol-3-yl)-5-t-butyloxy carbonylpyrrole-3-one	−7.56	−0.22	2.88	GLY536
6	4á,5à-dimethyl-3-methylene-1-azabicyclo[3.2.0]heptan-7-one	−5.6	−0.51	79.01	ASN537,VAL228

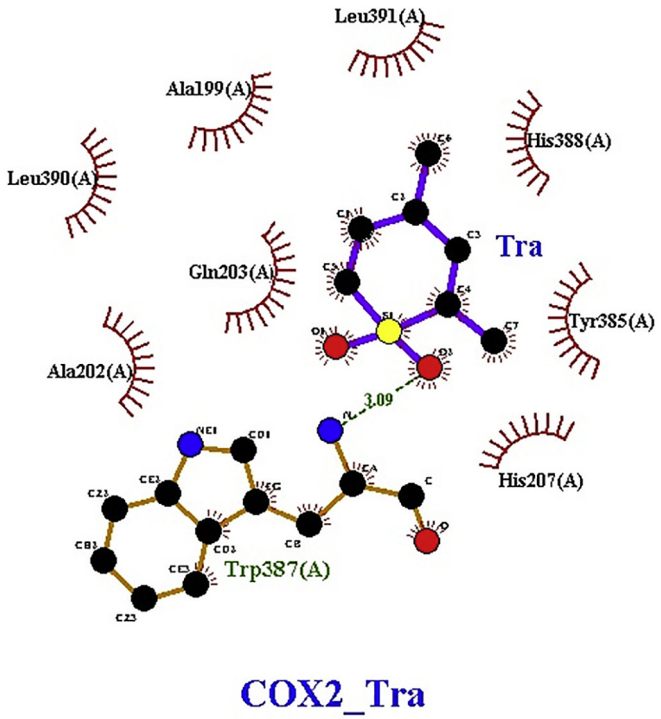

Fig. 8. Interaction of the COX-2 protein with Trans-2, 4-Dimethylthiane, S,S-dioxide.

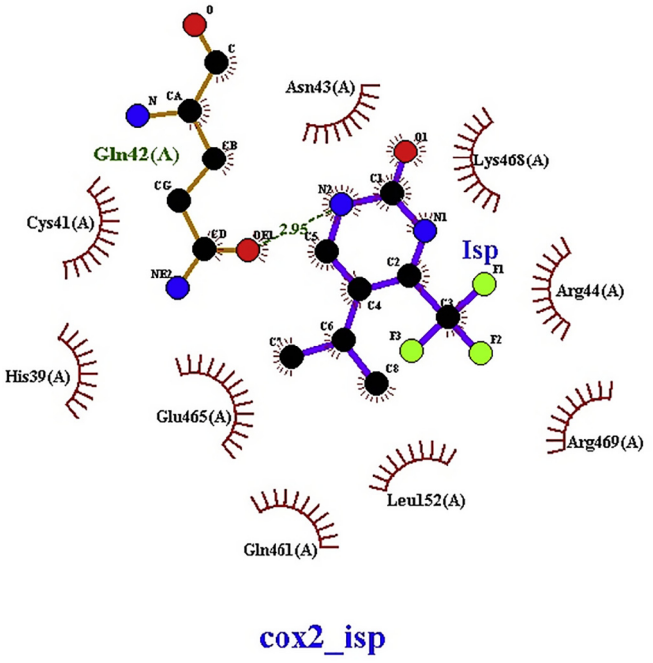

Fig. 9. Interaction of the COX-2 protein with 5-Isopropyl-4- (trifluoromethyl)-1H-pyrimidine-2-one.

150ARG, 151ALA, 152LEU, 153PRO, 154PRO, 155VAL, 156PRO, 157ASP, 192GLN, 205PHE, 206THR, 209PHE, 227GLY, 228VAL, 344VAL, 345ILE, 348TYR, 349VAL, 352LEU, 353SER, 355TYR, 357PHE, 359LEU, 370GLN, 371PHE, 372GLN, 374GLN, 375ASN, 376ARG, 377ILE, 378ALA, 381PHE, 384LEU, 385TYR, 387TRP, 459LYS, 461GLN, 465GLU, 468LYS, 469ARG, 470PHE, 471MET, 472LEU, 513ARG, 516ALA, 517ILE, 518PHE, 522MET, 523VAL, 524GLU, 526GLY, 527ALA, 529PHE, 530SER, 531LEU, 532LYS, 533GLY, 534LEU. The orientation of compounds in the binding pocket and their interacting residues have been depicted in Table 4. All of the active sites illustrated in the binding pocket region were selected for further docking analysis.

Out of all the six compounds used for docking analysis, (1-Benzyl-3-isopropyl-5-(1-allylindol-3-yl)-5-t-butyloxy carbonylpyrrole-3-one) depicted a least binding energy of (−7.56 kcal/mol); i.e. highest binding affinity toward the COX-2 protein. Two-dimensional intermolecular interaction of the compounds and the protein molecule was visualized using LigPlot ver. 2.1. The K_i value of (1-Benzyl-3-isopropyl-5-(1-allylindol-3-yl)-5-t-butyloxy carbonylpyrrole-3-one) is least, which indicates that only 2.88 of the compound is required to decrease the activity of the gene by half fold (see Figs. 8 and 9).

Ten different conformations were generated when Photocitral A was

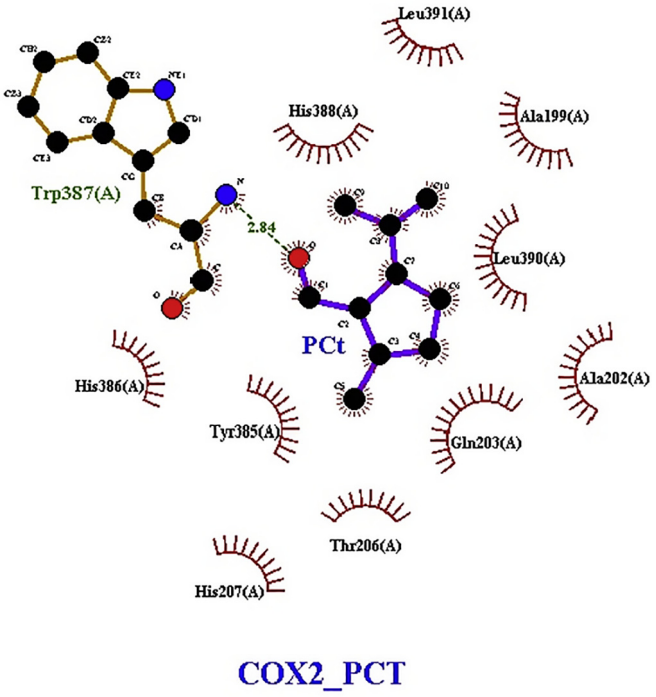

Fig. 10. Interaction of the COX-2 protein with Photocitral A.

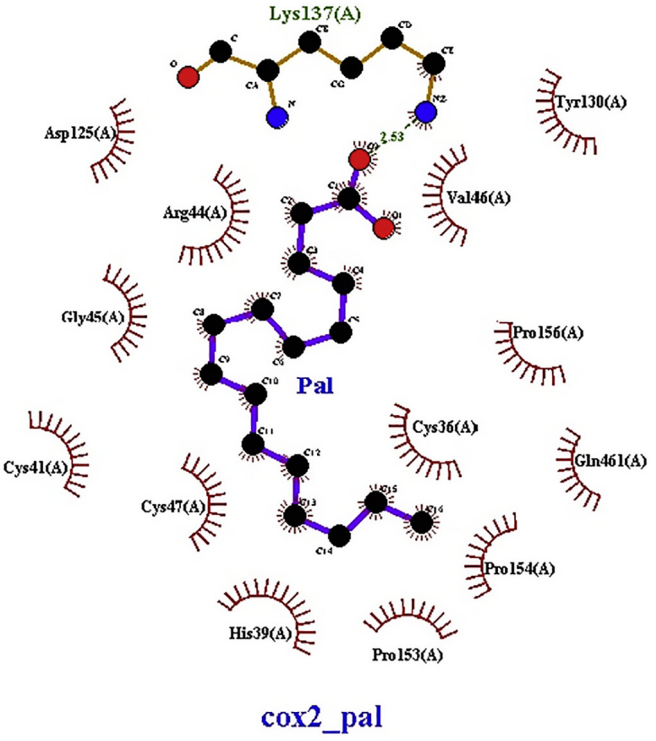

Fig. 11. Interaction of the COX-2 protein with Palmitic acid.

docked with COX-2, among which best-docked complex was considered for binding score determination. A binding score of (−6.36) and ligand efficiency of (−0.58) was obtained with one hydrogen bond formed with Trp387, and the bond length was 2.84 (Fig. 10) (see Figs. 11-13).

4. Conclusion

The current study revealed that bioactive phyto-compounds of

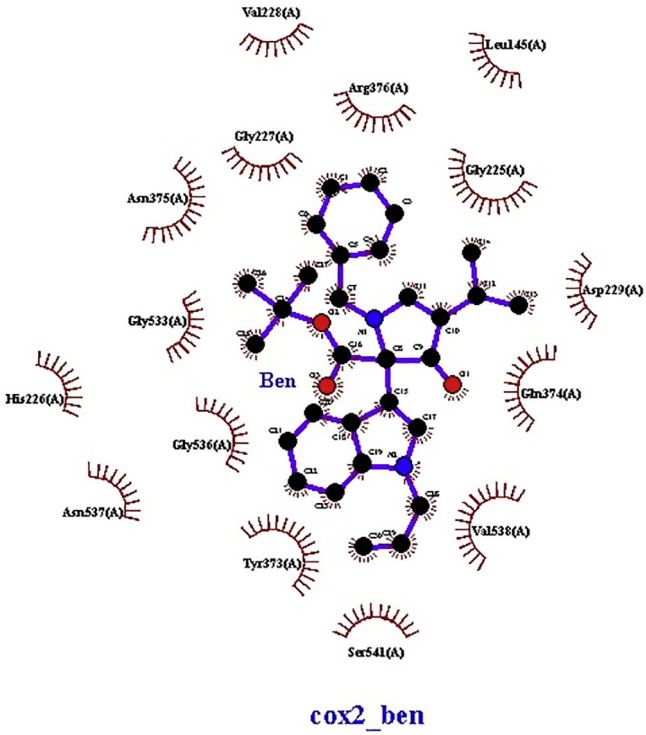

Fig. 12. Interaction of the COX-2 protein with 1- Benzyl-3-isopropyl-5-(1-allylindol-3-yl)-5-t-butyloxy carbonylpyrrole- 3- one.

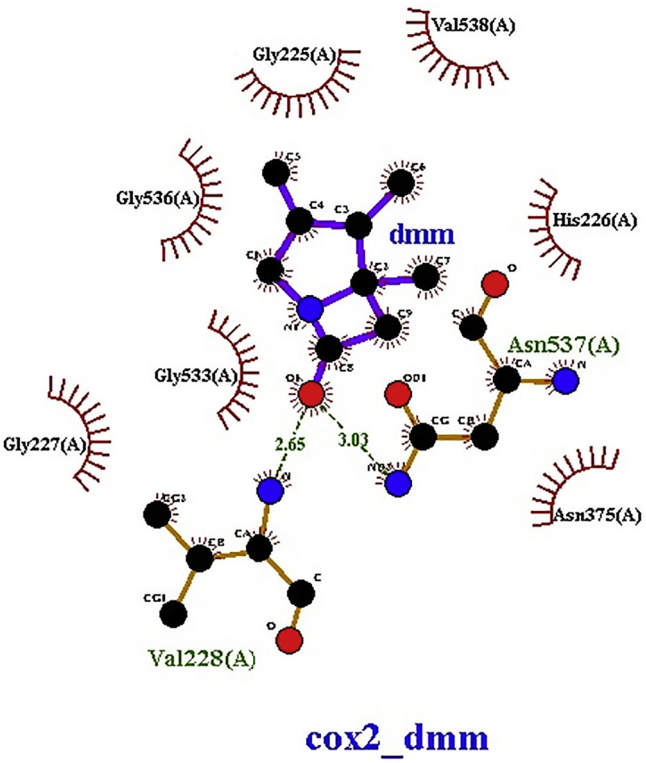

Fig. 13. Interaction of the COX-2 protein with 4á, 5à-dimethyl-3-methylene-1-azabicyclo [3.2.0] heptan-7-one.

Kalanchoe pinnata methanol extract possess potent anti-inflammatory activity. The MTT assay depicted the biocompatible nature of methanol extract in different concentrations. All the compounds were effectively docked against a common inflammation therapeutic target i.e. COX-2

for drug development and research. This combinatorial analysis approach of anti-inflammatory activity screening (in-vitro anti-inflammatory activity testing using inhibition of albumin denaturation assay, anti-proteinase activity assay, heat and hypotonicity induced hemolysis assay and in-silico molecular docking validation) can be helpful for designing phyto-compounds as novel drug candidates for the treatment of inflammatory disorders.

Acknowledgements

The author would like to thank Vellore Institute of Technology (VIT) for providing the seed money to carry out the research work.

References

[1] Pendota SC, Ndhlala AR, Aremu AO, Aderogba MA, Van Staden J. Anti-inflammatory, antioxidant and in silico studies of Buddleja salviifolia (L). Lam leaf constituents. South Afr J Bot 2014;93:79–85. https://doi.org/10.1016/j.sajb.2014.03.012.

[2] Ashraf Z, Alamgeer, Kanwal M, Hassan M, Abdullah S, Waheed M, et al. Flurbiprofen–antioxidant mutual prodrugs as safer nonsteroidal anti-inflammatory drugs: synthesis, pharmacological investigation, and computational molecular modeling. Drug Des Dev Ther 2016;10:2401–19. https://doi.org/10.2147/DDDT.S109318.

[3] Amaravani M, Prasad NK, Ramakrishna V. COX-2 structural analysis and docking studies with gallic acid structural analogues. SpringerPlus 2012;1:1–7. https://doi.org/10.1186/2193-1801-1-58.

[4] Cao H, Yu R, Choi Y, Ma ZZ, Zhang H, Xiang W, et al. Discovery of cyclooxygenase inhibitors from medicinal plants used to treat inflammation. Pharmacol Res 2010;61:519–24. https://doi.org/10.1016/j.phrs.2010.02.007.

[5] Szajwaj BM, Pecio L, Kowalczyk M, AS. New bufadienolides isolated from the roots of Kalanchoe daigremontiana (Crassulaceae). Molecules 2016;21:243. https://doi.org/10.3390/molecules21030243.

[6] Muzitano MF, Tinoco LW, Guette C, Kaiser CR, Costa S. The antileishmanial activity assessment of unusual flavonoids from Kalanchoe pinnata. Phytochemistry 2006;67:2071–7. https://doi.org/10.1016/j.phytochem.2006.06.027.

[7] Chaturvedi OS, Joshi A, BKD. Pharmacognostical, phytochemical evaluation and antiinflammatory activity of stem of Kalanchoe pinnata. Int J Pharma Sci Res 2012;3:1133–40.

[8] Govindappa M, Channabasava R, Dv S, Meenakshi J, Lavanya A, Santoyo G, et al. Phytochemical screening , antimicrobial and in vitro anti-inflammatory activity of endophytic extracts from Loranthus sp. Pharm J 2011;3:82–90. https://doi.org/10.5530/pj.2011.25.15.

[9] Chandra S, Chatterjee P, Dey P, Bhattacharya S. Evaluation of anti-inflammatory effect of Ashwagandha : a preliminary study in vitro. Pharm J 2012;4:47–9. https://doi.org/10.5530/pj.2012.29.7.

[10] Morinda F, Linn C, Reference W, Alzheimer TO. Insilco identification of suitable acetuylcholinesterase inhibitors from morinda citrifolia linn. with reference to alzheimer's disease Kukkarasapalli Praveen and Kuna Yellamma* Department of Zoology, Sri Venkateswara University, Tirupati-517502, Andhra. Int J Pharma Sci Res 2014;5:5474–81. https://doi.org/10.13040/IJPSR.0975-8232.5(12).5474-81.

[11] Pratama SF, Muda AK, Choo YH, Abraham A. Preparation of ATS drugs 3D molecular structure for 3D moment invariants-based molecular descriptors. Adv Intell Syst Comput 2018;734:252–61. https://doi.org/10.1007/978-3-319-76351-4_26.

[12] Pedretti A, Villa L, Vistoli G. VEGA: A versatile program to convert, handle and visualize molecular structure on Windows-based PCs. J Mol Graph Model 2002;21:47–9. https://doi.org/10.1016/S1093-3263(02)00123-7.

[13] Asati V, Bajaj S, Mahapatra DK, Bharti SK. Molecular modeling studies of some thiazolidine-2,4-dione derivatives as 15-PGDH inhibitors. Med Chem Res 2016;25:94–108. https://doi.org/10.1007/s00044-015-1442-5.

[14] Gudgila R, Leclerc CA. Combining molecular docking and molecular dynamics to predict the binding modes of flavonoid derivatives with the neuraminidase of the 2009 H1N1 influenza a Virus Shih-Jen. Int J Mol Sci 2012;13:4496–507. https://doi.org/10.3390/ijms13044496.

[15] Sulimov VB, Katkova EV, Oferkin IV, Sulimov AV, Romanov AN, Roschin AI, et al. Application of molecular modeling to urokinase inhibitors development. BioMed Res Int 2014:1–15. https://doi.org/10.1155/2014/625176.

[16] Binkowski TA, Naghibzadeh S, Liang J. CASTp: computed Atlas of surface Topography of proteins. Nucleic Acids Res 2003;31:3352–5. https://doi.org/10.1093/nar/gkg512.

[17] Tiwary BK, Pathak RK, Pradhan K, Nanda AK, Kumar A, Chakraborty R. Evaluation of drug candidature of some quinazoline- 4-(3h)-ones as inhibitor of human dihydrofolate reductase enzyme: molecular docking and in silico studies. Int J Pharm Pharmaceut Sci 2014;6:393–400.

[18] Wallace AC, Laskowski RA, Thornton JM. LIGPLOT : a program to generate schematic diagrams of protein-ligand interactions. Protein Eng 1995;8:127–34.

[19] Phatak RS. GC-MS analysis of bioactive compounds in the methanolic extract of Kalanchoe pinnata fresh leaves. J Chem Pharmaceut Res 2015;7:34–7.

[20] Perumal R, Dey A, Manavalan R, Prakasam K, Jayachandra E, Sreenivasa G. Inhibition of albumin denaturation and anti inflammatory activity of furfuryl substituted pyrimidinoimidazolinones. Int J Chem Sci 2008;6:2016–22.

[21] Elisha IL, Dzoyem J, Mcgaw LJ, Botha FS, Eloff JN. The anti-arthritic, anti-inflammatory,antioxidant activity and relationships with total phenolics and total flavonoids of nine South African plants used traditionally to treat arthritis. BMC Complement Altern Med 2016;16:1–10. https://doi.org/10.1186/s12906-016-1301-z.

[22] Naz R, Ayub H, Nawaz S, Islam ZU, Yasmin T, Bano A, et al. Antimicrobial activity, toxicity and anti-inflammatory potential of methanolic extracts of four ethnomedicinal plant species from Punjab, Pakistan. BMC Complement Altern Med 2017;17:1–13. https://doi.org/10.1186/s12906-017-1815-z.

[23] Anosike CA, Obidoa O, Ezeanyika LUS. Membrane stabilization as a mechanism of the anti-inflammatory activity of methanol extract of garden egg (Solanum aethiopicum). DARU J Pharm Sci 2012;20:1. https://doi.org/10.1186/2008-2231-20-76.

[24] Halliwell B, Whiteman M. Measuring reactive species and oxidative damage in vivo and in cell culture : how should you do it and what do the results mean ? Br J Pharmacol 2004;142:231–55. https://doi.org/10.1038/sj.bjp.0705776.

[25] Asirvatham R, Christina AJM, Murali A. In vitro antioxidant and anticancer activity studies on drosera indica L. (droseraceae). Adv Pharmaceut Bull 2013;3:115–20. https://doi.org/10.5681/apb.2013.019.

[26] Ahmad N, Sharma S, Singh VN, Shamsi SF, Fatma A, Mehta BR. Biosynthesis of silver nanoparticles from Desmodium triflorum : a novel approach towards weed utilization 2011. 2011. https://doi.org/10.4061/2011/454090.

[27] Chella Perumal P, Sowmya S, Pratibha P, Vidya B, Anusooriya P, Starlin T, et al. Identification of novel PPARγ agonist from GC-MS analysis of ethanolic extract of Cayratia trifolia (L.): a computational molecular simulation studies. J Appl Pharmaceut Sci 2014;4:6–11. https://doi.org/10.7324/JAPS.2014.40902.

[28] Raghunath M, Singh A, Viswanathan CL. Molecular descriptors and bioactivity scores of 6- substituted benzimidazole-2-carbamates as potential anticancer agents. World J Pharm Pharmaceut Sci 2015;4:1438–45.

[29] Khan S, Kumar S, Maqsood A. Virtual screening of molecular properties and bioactivity score of boswellic acid derivatives in search of potent anti-inflammatory lead molecule. Int J Interdiscip Multidiscip Stud 2013;1:8–12.

[30] Verma A. Lead finding from Phyllanthus debelis with hepatoprotective potentials. Asian Pac J Trop Biomed 2012;2:1735–7. https://doi.org/10.1016/S2221-1691(12)60486-9.